Event-Triggered Formation Tracking Control With Application to Multiple Mobile Robots

Zipeng Huang, *Student Member, IEEE*, Robert Bauer, and Ya-Jun Pan, *Senior Member, IEEE*

***Abstract*—In this article, we address the distributed event-triggered leader–follower formation tracking control problem of general linear multiagent systems with a dynamic leader in sampled-data settings. A novel locally computable state-estimate-based event generator is established for each follower agent to regulate the interagent communication at each sampling instant. Then, we propose a distributed formation tracking protocol based on the triggered sampled information such that the formation tracking control problem can be formulated as a stability-analysis problem of the closed-loop formation error dynamics. The event generator and formation tracking controller gains can then be co-designed using the feasible linear matrix inequality conditions that are derived from Lyapunov-based stability-analysis methods that guarantee the ultimate boundedness of the closed-loop formation error dynamics. Finally, numerical simulations along with experiment implementations were conducted for a group of linearized unicycle-type mobile robots to demonstrate the effectiveness and advantages of the proposed method.**

***Index Terms*—Dynamic leader, event-triggered control (ETC), formation control, mobile robots, sampled-data control.**

I. Introduction

In RECENT years, inspired by the formation tactics of biological systems, such as birds migrating in a V-shaped formation to improve aerodynamic efficiency, researchers have applied formation strategies to multirobotic systems to accomplish various tasks including payload transportation, object searching, and forest fire monitoring. Formation control strategies in multiagent systems (MASs) are recognized as formation tracking design or formation producing design depending on whether there is a group reference [1]. Early formation control methods, such as virtual structure [2] and behavior based [3], have been found to be successful in handling complex formation tasks subject to various constraints and agent dynamics; however, centralized implementation is often required in those approaches, which makes them less applicable for large-size agent teams. In addition, the closed-loop system stability is difficult to mathematically prove, and the system convergence is often not guaranteed.

Following the early successes of applying the consensus theory to the formation control of multiple mobile robots in [4], researchers have devoted a tremendous amount of effort to developing distributed convergence-guaranteed formation controllers. For integrator-type systems, based on the invariant displacement, distance, or bearing constraints that are employed to establish the desired group formation, the consensus-based formation approaches can be accordingly categorized as displacement based, distance based, or bearing based [5]. Formation control problems for MASs with more complex agent dynamics have also been investigated in the literature. For example, the formation tracking control problem has been studied for MAS with general linear agents and a nonautonomous leader [6]. A multilayer framework was adopted to study the formation control of multiple Euler–Lagrange systems in [7]. Finite-time formation controllers were proposed in [8] for a group of quadcopter agents. Time-varying formation producing [9] and formation tracking [10] for general heterogeneous linear MASs have also been investigated in the literature.

It should be noted that most of the existing works in the literature, including the aforementioned ones, consider continuous or regular equally spaced (periodic) communication in the formation control protocol design, which is generally impractical and inefficient since all communication networks have limited bandwidth. For instance, it is unrealistic to apply continuous formation protocols to a group of underwater rovers since the underwater network has a very low data transmission rate. Therefore, it is important to take into account the limited communication resources in a formation controller design. Recently, event-triggered control (ETC) strategies [11]–[15] have gained popularity in addressing limited communication resources in networked control systems. The underlying idea in ETC is to have agents broadcast and update their sampled states only when certain predesigned triggering conditions are satisfied. Therefore, it is possible to reduce communication resource consumption while still maintaining comparable performances by properly designing the triggering rules. Yin *et al.* [16] and Garcia *et al.* [17] studied the consensus tracking problem for general linear multi-agent system (MAS). The leaderless formation control problem of general linear MAS was addressed in [18]. Notwithstanding the advantages of ETC strategies, analytically excluding Zeno behavior associated with the proposed triggering rules is often a challenge. Among many

Manuscript received 17 September 2021; revised 31 December 2021; accepted 16 January 2022. Date of publication 1 February 2022; date of current version 22 August 2022. This work was supported in part by NSERC, Government of Nova Scotia, and in part by Dalhousie University. *(Corresponding author: Ya-Jun Pan.)*

The authors are with the Department of Mechanical Engineering, Dalhousie University, Halifax, NS B3H 4R2, Canada (e-mail: zz794020@dal.ca; robert.bauer@dal.ca; yajun.pan@dal.ca).

This article has supplementary material provided by the authors and color versions of one or more figures available at https://doi.org/10.1109/TIE.2022.3146582.

Digital Object Identifier 10.1109/TIE.2022.3146582

ETC schemes, the sampled-data-based ETC scheme [19], where triggering conditions are tested at each sampling instant, naturally rules out Zeno behavior since the minimum interevent time is lower bounded by the sampling interval.

Motivated by the abovementioned discussion, the present article addresses the formation tracking control problem for general linear MASs with a dynamic nonautonomous leader using a sampled-data-based ETC scheme. The contributions of this article are at least threefold.

1) First, compared with the continuous ETC mechanisms, the formation tracking control algorithm proposed under a sampled-data-based setting in this work is more economical and realistic since communication events on all agents will only be evaluated at each sampling instant.
2) Second, different from the leaderless formation control design using a state-error-based event-triggered communication mechanism (ECM) in [18], this work studies the more general leader–follower formation tracking problem using a novel estimate-error-based ECM.
3) Finally, the proposed method was first verified in simulations and then implemented experimentally on a group of Pioneer mobile robots. It was shown in both simulation and experiment that the proposed novel estimate-error-based ECM can effectively reduce communication resource usage while still providing comparable performance.

The rest of this article is organized as follows. Section II presents the preliminary concepts and develops the formation control problem. A distributed formation controller along with a communication-event generator is proposed in Section III. Sufficient conditions for the controller gain and triggering-condition gain design are also provided in this section. Section IV illustrates the proposed design method through both simulation and experiment studies. Section V concludes this article and makes recommendations for future research.

Notation: Throughout this article, $\mathbf{I}_N$ represents an identity matrix with dimension N, the superscript T stands for matrix transposition, and $\otimes$ is the Kronecker product sign. Furthermore, $\|x\|$ denotes the Euclidean norm of a vector $x \in R^n$, and $\text{diag}\{a_1, \ldots, a_n\}$ represents a diagonal matrix with $a_1, \ldots, a_n$ as its diagonal elements. The symmetric element of a block symmetric matrix is denoted by $*$. $|\mathcal{N}|$ denotes the cardinality of the set $\mathcal{N}$.

II. Problem Formulation

A. Graph Theory

Let $\mathcal{G}(\mathcal{V}, \mathcal{E})$ denotes a directed graph with a set of nodes $\mathcal{V}$ and a set of edges $\mathcal{E}$. An edge $(j, i) \in \mathcal{E}$ indicates that Agent i receives information from Agent j, in which case node j is called a neighbor of node i, and $\mathcal{N}_i$ denotes the neighboring set of node i. Edges in undirected graphs are bidirectional, i.e., $(i, j) \in \mathcal{E}$ implies $(j, i) \in \mathcal{E}$. A directed path from nodes i_1 to i_k is a sequence of ordered edges of the form $(i_l, i_{l+1}),\ l = 1, \ldots, k-1$. The adjacency matrix $\mathcal{A} = [a_{ij}]$ of a graph is defined such that $a_{ij} = 1$ if $(j, i) \in \mathcal{E}$ and $a_{ij} = 0$, otherwise. The associated diagonal in-degree matrix $\mathcal{D}$ is given as $d_{ii} = \sum_{j=1}^{N} a_{ij}, i = 1, \ldots, N$, and the Laplacian matrix $\mathcal{L}$ can be defined as $\mathcal{L} = \mathcal{D} - \mathcal{A}$. For a leader–follower type communication topology, define L_{ff} as $\mathcal{L} + \text{diag}\{d_1, \ldots, d_N\}$, where $\mathcal{L}$ is the Laplacian matrix among followers and d_i is 1 if the leader's information is accessible to the ith follower and 0, otherwise.

Assumption 1: The leader has a directed path to all follower agents. As such, L_{ff} is nonsingular and, hence, invertible [1].

B. Problem Formulation

Consider a group of N identical follower agents and one leader agent described by

$$\dot{\mathbf{x}}_i = A\mathbf{x}_i + B\mathbf{u}_i,\ i = 1, \ldots, N \tag{1a}$$

$$\dot{\mathbf{x}}_0 = A\mathbf{x}_0 + B\mathbf{u}_0 \tag{1b}$$

where $\mathbf{x}_i \in R^n$ denotes the follower's state, $\mathbf{x}_0 \in R^n$ is the leader's state, $\mathbf{u}_0$ is the leader's control input, and $\mathbf{u}_i \in R^m$ is the followers' control input to be designed. A and B are known system and control matrices with compatible dimensions. In addition, B is assumed to have full column rank.

Definition 1: The formation control problem for the leader–follower MAS (1) is solved with bounded error if the formation error vectors $\eta_i = \mathbf{x}_i - f_i - \mathbf{x}_0$ satisfy the following condition:

$$\lim_{t\to\infty} \|\boldsymbol{\eta}_i\| \le \sigma,\ i = 1, \ldots, N \tag{2}$$

where σ is a small positive tunable parameter, and f_i is a constant predesigned formation vector that characterizes the desired relative position of Agent i with respect to the leader.

Remark 1: In the special case that $f_i = 0$ for all $i \in \mathcal{V}$, the formation tracking control problem is reduced to a leader–follower tracking problem.

Unlike traditional formation control designs for System (1) using either continuous communication or continuous ECM schemes that are inefficient or impractical in hardware implementation, the formation control problem is studied under a sampled-data environment from a practical implementation point of view in this article. While the individual agents' control system is sampled at a periodic rate (having regular equally spaced sampling instants), the interagent communication is governed by some predesigned triggering conditions, which are evaluated at each sampling instant. In other words, an agent broadcasts its sampled states to its neighbors only when certain conditions are met. The objective of this work is, then, to develop a distributed locally computable control law and an ECM such that the formation control for System (1) with a communication topology satisfying Assumption 1 can be achieved with bounded error. The following lemma will be used in the sufficient condition formulation in Section III-D:

Lemma 1 ([20]): Given a positive definite matrix $R \in R^{n\times n}$, if there exists an arbitrary matrix $S \in R^{n\times n}$ such that

$$\begin{bmatrix} R & * \\ S^T & R \end{bmatrix} \ge 0 \tag{3}$$

then for any $\tau \in [0, h]$, the following inequality holds:

$$\begin{aligned} -h\int_{t-h}^{t} \dot{\eta}^T(v)(\mathbf{I}_N \otimes R)\dot{\eta}(v)dv \\ \leq -\phi_1^T(\mathbf{I}_N \otimes R)\phi_1 - \phi_2^T(\mathbf{I}_N \otimes R)\phi_2 \\ - \phi_1^T(\mathbf{I}_N \otimes S)\phi_2 - \phi_2^T(\mathbf{I}_N \otimes S^T)\phi_1 \end{aligned} \tag{4}$$

where $\phi_1 = \eta(t-\tau) - \eta(t)$ and $\phi_2 = \eta(t-h) - \eta(t-\tau)$.

III. Main Results

A distributed sampled-data-based controller along with an state-estimate-based ECM are proposed to address the formation control problem in this section.

A. Controller Design

For $t \in [vh, (v+1)h)$, a distributed formation control input for Agent $i = 1, \ldots, N$ is proposed as

$$\begin{aligned} \mathbf{u}_i(t) = \frac{K}{|\mathcal{N}_i|}\sum_{j=1}^{N} a_{ij}(\hat{\mathbf{x}}_i(vh) - \hat{\mathbf{x}}_j(vh) - f_i + f_j) - \frac{\mu_i}{|\mathcal{N}_i|} \\ + \frac{K}{|\mathcal{N}_i|}a_{i0}(\hat{\mathbf{x}}_i(vh) - f_i - \mathbf{x}_0) + \frac{\sum_{j=1}^{N} a_{ij}}{|\mathcal{N}_i|}\mathbf{u}_j(t_{k'}^j h) \\ + \frac{a_{i0}}{|\mathcal{N}_i|}\mathbf{u}_0(vh) \end{aligned} \tag{5}$$

where μ_i is the formation compensation input to be determined, and $\hat{\mathbf{x}}_i(vh)$ and $\hat{\mathbf{x}}_j(vh)$ are the estimated states of Agents i and j at the latest sampling instant vh. For follower agents $i = 1, \ldots, N$, the sate estimators follow the dynamics $\dot{\hat{x}}_i = A\hat{x}_i + B\mathbf{u}_i(t_{\tilde{k}}^i h), t \in [t_{\tilde{k}}^i h, (t_{\tilde{k}}^i + 1)h)$, and $\hat{x}_i(t_{\tilde{k}}^i h) = x_i(t_{\tilde{k}}^i h)$, where $t_{\tilde{k}}^i h$ and $(t_{\tilde{k}}^i + 1)h$ represent the latest released and next triggering (available to their neighbors) sampling instants for Agent i, respectively. K is a static gain matrix that will be designed based on the sufficient conditions that ensure system stability. Moreover, it was shown in [6] that there exists a nonsingular matrix $\mathrm{Y} = \left[\tilde{B}^T, \bar{B}^T\right]^T$, where $\tilde{B}B = \mathbf{I}_m$ and $\bar{B}B = 0_{n-m}$ for a full-column rank matrix B. μ_i can then be designed as $\tilde{B}A\sum_{j=0}^{N} a_{ij}(f_i - f_j)$.

Remark 2: In addition to the formation tracking controller proposed in [21], the controller (5) also utilizes the control input information from neighboring agents. As a result, the final group formation error bound will be independent of the bound of the leader's input. It is possible to design formation controllers without using neighbors' input information given that the leader's input is bounded as $\|\mathbf{u}_0\| \leq \bar{u}$, where $\bar{u}$ is a known positive constant. For this case, sufficient linear matrix inequality (LMI) conditions can also be derived that guarantee the asymptotic convergence of formation error to a neighborhood of the origin defined by $\bar{u}$.

B. Closed-Loop Dynamics

The networked closed-loop dynamics of Agent i under input (5) satisfying the following equation for $t \in [vh, (v+1)h)$ is given by

$$\begin{aligned} \sum_{j=0}^{N} a_{ij}B(\mathbf{u}_i(t) - \mathbf{u}_j(t)) = \sum_{j=0}^{N} a_{ij}BK(e_i(vh) - e_j(vh) \\ + \sum_{j=0}^{N} a_{ij}BK(\eta_i(vh) - \eta_j(vh)) + \sum_{j=1}^{N} a_{ij}\bar{e}_j(vh) - B\mu_i \end{aligned} \tag{6}$$

where $\mathbf{e}_i(vh) = \hat{\mathbf{x}}_i(vh) - \mathbf{x}_i(vh)$ and $\mathbf{e}_j(vh) = \hat{\mathbf{x}}_j(vh) - \mathbf{x}_j(vh)$ denote the state estimation error for Agents i and j at the sampling instant vh, respectively. In addition, $\bar{e}_i(vh) = \mathbf{u}_i(t_k^i h) - \mathbf{u}_i(vh)$ denotes the control input error at the sampling instant vh. Substituting the system dynamics (1) into (6) yields

$$\begin{aligned} \sum_{j=0}^{N} a_{ij}\dot{x}_i(t) = \sum_{j=0}^{N} a_{ij}\dot{x}_j(t) + \sum_{j=0}^{N} a_{ij}BK(e_i(vh) - e_j(vh)) \\ + \sum_{j=0}^{N} a_{ij}BK(\eta_i(vh) - \eta_j(vh)) + \sum_{j=1}^{N} a_{ij}\bar{e}_j(vh) \\ + \sum_{j=0}^{N} a_{ij}(Ax_i(t) - Ax_j(t) - Af_i + Af_j) \\ + \sum_{j=0}^{N} a_{ij}(Af_i - Af_j) - B\mu_i. \end{aligned} \tag{7}$$

Assumption 2: $\bar{B}Af_i = 0,\ i = 1, \ldots, N$ is satisfied.

It can be verified that $Af_i = B\tilde{B}Af_i$ and the term $\sum_{j=0}^{N} a_{ij}(Af_i - Af_j) - B\mu_i$ is nullified under Assumption 2. In addition, $\dot{x}_i - \dot{x}_j = \dot{\eta}_i - \dot{\eta}_j$ since f_i is a constant. Therefore, (7) is reduced to

$$\begin{aligned} \sum_{j=0}^{N} a_{ij}\dot{\eta}_i(t) = \sum_{j=0}^{N} a_{ij}\dot{\eta}_j(t) + \sum_{j=0}^{N} a_{ij}BK(e_i(vh) - e_j(vh)) \\ + \sum_{j=0}^{N} a_{ij}BK(\eta_i(vh) - \eta_j(vh)) + \sum_{j=1}^{N} a_{ij}\bar{e}_j(vh) \\ + \sum_{j=0}^{N} a_{ij}A(\eta_i(t) - \eta_j(t)). \end{aligned} \tag{8}$$

Definition 2: Define $\tau(t) = t - vh,\ t \in [vh, (v+1)h)$ as an artificial system delay. Then, the latest sampled instance vh can be replaced by $t - \tau(t)$. In addition, the time variable in $\tau(t)$ will be neglected for brevity hereafter.

Under the abovementioned assumptions and definitions, the overall closed-loop formation error dynamics become

$$\begin{aligned} \dot{\boldsymbol{\eta}}(t) = (\mathbf{I}_N \otimes BK)\mathbf{e}(t-\tau) + (\mathbf{I}_N \otimes BK)\boldsymbol{\eta}(t-\tau) \\ + (\mathbf{I}_N \otimes A)\eta(t) + (L_{ff}^{-1}\mathcal{A}_f \otimes B)\bar{\mathbf{e}}(t-\tau) \end{aligned} \tag{9}$$

where $\mathcal{A}_f$ denotes the adjacency matrix among the follower agents, and $\boldsymbol{\eta}(t-\tau)$, $\mathbf{e}(t-\tau)$, and $\bar{\mathbf{e}}(t-\tau)$ are the stacked form of $\eta_i(t-\tau)$, $e_i(t-\tau)$, and $\bar{e}_i(t-\tau)$, respectively.

C. Event Generator Design

Inspired by the idea of combined measurements [22], we define the combined formation error for Agent i as

$$\begin{aligned} q_i(vh) &= \sum_{j=1}^{N} a_{ij}(\hat{x}_i(vh) - \hat{x}_j(vh) - f_i + f_j) \\ &\quad + a_{i0}(\hat{x}_i(vh) - f_i - x_0) \\ &= \sum_{j=0}^{N} a_{ij}(\eta_i(vh) + e_i(vh) - \eta_j(vh) - e_j(vh)). \end{aligned} \tag{10}$$

Then, a triggering function for Agent i at instant vh can be designed as

$$\begin{aligned} f_i(vh) = e_i(vh)^T \Psi_1 e_i(vh) + \bar{e}_i^T(vh)\Psi_2 \bar{e}_i^T(vh) \\ - q_i(vh)^T \Phi q_i(vh) - \epsilon^2 \end{aligned} \tag{11}$$

where Ψ_1, Ψ_2, and Φ are the positive definite matrices to be determined, and ϵ is a small positive design parameter. The next event release instant for Agent i can then be determined as follows:

$$t_{k+1}^i h = \inf\{vh > t_k h |\ f_i(vh) > 0\}. \tag{12}$$

It should be noted that the event generator on each agent is designed based on its neighbors' estimated state information. Specifically, each agent estimates its neighbors' current state information based on their previously triggered state information using model-based closed-loop estimators. Therefore, the neighbors' true state information is not used in triggering function evaluations on sampling instants, and the communication cost can be reduced. It addition, the state estimate error $e_i(vh)$ and control input error $\bar{e}_i(vh)$ are reset to zero whenever interagent communications are enabled, which happens when triggering rules (12) are activated. Therefore, $f_i(vh) \le 0$ can be enforced for all agents at all sampling instants, which implies that $\sum_{i=1}^{N} f_i(vh) \le 0$ is always satisfied. From (11),

$$\begin{aligned} &\sum_{i=1}^{N} f_i(vh) \\ &= \sum_{i=1}^{N} (e_i(vh)^T \Psi_1 e_i(vh) + \bar{e}_i^T(vh)\Psi_2 \bar{e}_i^T(vh) \\ &\quad - q_i(vh)^T \Phi q_i(vh) - \epsilon^2) \\ &= \sum_{i=1}^{N} e_i(vh)^T \Psi_1 e_i(vh) + \sum_{i=1}^{N} \bar{e}_i^T(vh)\Psi_2 \bar{e}_i^T(vh) - N\epsilon^2 \\ &\quad - \sum_{i=1}^{N} \left[\sum_{j=0}^{N} a_{ij}(\eta_i(vh) + e_i(vh) - \eta_j(vh) - e_j(vh)^T) \right] \Phi \\ &\quad \times \left[\sum_{j=0}^{N} a_{ij}(\eta_i(vh) + e_i(vh) - \eta_j(vh) - e_j(vh)) \right] \le 0 \end{aligned} \tag{13}$$

which can be rewritten as

$$\begin{aligned} &\begin{bmatrix} \mathbf{e}(t-\tau) \\ \boldsymbol{\eta}(t-\tau) \\ \bar{\mathbf{e}}(t-\tau) \end{bmatrix}^T \begin{bmatrix} \mathbf{I}_N \otimes \Psi_1 - L_{ff}^T L_{ff} \otimes \Phi & * & * \\ -L_{ff}^T L_{ff} \otimes \Phi & -L_{ff}^T L_{ff} \otimes \Phi & * \\ 0 & 0 & \mathbf{I}_N \otimes \Psi_2 \end{bmatrix} \\ &\qquad \begin{bmatrix} \boldsymbol{\eta}(t-\tau) \\ \mathbf{e}(t-\tau) \\ \bar{\mathbf{e}}(t-\tau) \end{bmatrix} \le N\epsilon^2 \end{aligned} \tag{14}$$

where 0 denotes a zero matrix with compatible dimensions.

Remark 3: State errors have been commonly used in triggering condition design in the literature [18] and [23]; however, state-error-based event generators tend to produce frequent communication instants in the presence of a dynamic leader in the formation control even when the desired formation has been achieved. An estimate-error-based event generator is, therefore, used in this article with the aim to reduce triggering instants while still providing comparable formation performance. In addition, the small positive threshold ϵ is introduced to account for the numerical error associated with the triggering condition evaluations.

D. Main Results

The following theorem provides sufficient conditions for co-designing the event generator and formation controller gains.

Theorem 1: Under Assumptions 1 and 2, the control law (5) and the communication regulation condition given by (12), the system (1) achieves formation with bounded error if, for given positive scalars ρ and β, there exist symmetric positive definite matrices $\tilde{\Phi}$, $\tilde{\Psi}_1$, $\tilde{\Psi}_2$, $\tilde{P}$, $\tilde{Q}$, $\tilde{R} \in \mathbb{R}^{n\times n}$, as well as arbitrary matrices $\tilde{S} \in \mathbb{R}^{n\times n}$ and $Y \in \mathbb{R}^{m\times n}$, such that

$$\begin{bmatrix} \tilde{R} & * \\ \tilde{S}^T & \tilde{R} \end{bmatrix} \ge 0,\ H < 0 \tag{15}$$

where

$$\begin{bmatrix} H_{11} & * & * & * & * & * & * \\ H_{21} & H_{22} & * & * & * & * & * \\ H_{31} & H_{32} & H_{33} & * & * & * & * \\ H_{41} & H_{42} & 0 & H_{44} & * & * & * \\ H_{51} & 0 & 0 & 0 & H_{55} & * & * \\ H_{61} & H_{62} & 0 & H_{64} & 0 & H_{66} & * \\ H_{71} & 0 & 0 & 0 & 0 & 0 & H_{77} \end{bmatrix}$$

with

$$\begin{aligned} H_{11} &= \mathbf{I}_N \otimes (\tilde{P}A^T + A\tilde{P} \\ &\qquad + \tilde{Q} - \tilde{R}) \\ H_{21} &= \mathbf{I}_N \otimes (Y^T B^T + \tilde{R} - \tilde{S}^T) \\ H_{22} &= \mathbf{I}_N \otimes (-2\tilde{R} + \tilde{S} + \tilde{S}^T) \\ &\qquad + L_{ff}^T L_{ff} \otimes \tilde{\Phi} \\ H_{31} &= \mathbf{I}_N \otimes \tilde{S}^T \end{aligned}$$

$$H_{32} = \mathbf{I}_N \otimes (\tilde{R} - \tilde{S}^T)$$
$$H_{33} = -\mathbf{I}_N \otimes (\tilde{Q} + \tilde{R})$$
$$H_{41} = \mathbf{I}_N \otimes Y^T B^T$$
$$H_{42} = L_{ff}^T L_{ff} \otimes \tilde{\Phi}$$
$$H_{44} = -\mathbf{I}_N \otimes \tilde{\Psi}_1 + L_{ff}^T L_{ff} \otimes \tilde{\Phi}$$
$$H_{51} = \mathcal{A}^T L_{ff}^{-T} \otimes \tilde{P} B^T$$
$$H_{55} = -\mathbf{I}_N \otimes \tilde{\Psi}_2$$
$$H_{61} = h(\mathbf{I}_N \otimes A\tilde{P})$$
$$H_{62} = h(\mathbf{I}_N \otimes BY)$$
$$H_{64} = h(\mathbf{I}_N \otimes BY)$$
$$H_{65} = h(L_{ff}^{-1}\mathcal{A} \otimes B\tilde{P})$$
$$H_{66} = \rho^2(\mathbf{I}_N \otimes \tilde{R}) - 2\rho(\mathbf{I}_N \otimes \tilde{P})$$
$$H_{71} = \mathbf{I}_N \otimes \tilde{P}$$
$$H_{77} = -\frac{1}{\beta}\mathbf{I}_{Nn}.$$

Then, the controller gain K can be computed as $Y\tilde{P}^{-1}$, and the matrices Φ, Ψ_1, and Ψ_2 in the triggering conditions are obtained as $\tilde{P}^{-1}\tilde{\Phi}\tilde{P}^{-1}$, $\tilde{P}^{-1}\tilde{\Psi}_1\tilde{P}^{-1}$, and $\tilde{P}^{-1}\tilde{\Psi}_2\tilde{P}^{-1}$, respectively. In addition, the formation error is ultimately bounded as

$$\lim_{t\to\infty} \|\eta\| \le \sqrt{\frac{N}{\beta}}\epsilon. \tag{16}$$

Proof: Consider the following continuous Lyapunov function candidate on the interval $t \in [vh, (v+1)h)$ for the lumped formation error dynamics:

$$V(t) = V_1(t) + V_2(t) + V_3(t) \tag{17}$$

where

$$V_1(t) = \boldsymbol{\eta}(t)^T(\mathbf{I}_N \otimes P)\boldsymbol{\eta}(t)$$
$$V_2(t) = \int_{t-h}^{t} \boldsymbol{\eta}^T(s)(\mathbf{I}_N \otimes Q)\boldsymbol{\eta}(s)ds$$
$$V_3(t) = h\int_{t-h}^{t}\int_{s}^{t} \dot{\boldsymbol{\eta}}^T(v)(\mathbf{I}_N \otimes R)\dot{\boldsymbol{\eta}}(v)dvds$$

and $P, Q, R \in R^{n\times n}$ are symmetric positive definite matrices. Taking the time derivative of the Lyapunov function candidate along the overall system dynamics (9) yields

$$\dot{V}_1 = \eta(t)^T(\mathbf{I}_N \otimes (A^TP + PA))\eta(t) + 2\eta(t-\tau)^T(\mathbf{I}_N \otimes K^TB^TP)\eta(t) + 2\mathbf{e}(t-\tau)^T(\mathbf{I}_N \otimes K^TB^TP)\eta(t) + 2\bar{\mathbf{e}}(t-\tau)^T(\mathcal{A}_f^T L_{ff}^{-1} \otimes B^TP)\eta(t) \tag{18}$$

$$\dot{V}_2 = \eta^T(t)(\mathbf{I}_N \otimes Q)\eta(t) - \eta^T(t-h)(\mathbf{I}_N \otimes Q)\eta(t-h) \tag{19}$$

$$\dot{V}_3 = -h\int_{t-h}^{t} \dot{\eta}^T(v)(\mathbf{I}_N \otimes R)\dot{\eta}(v)dv + h^2\dot{\eta}^T(t)(\mathbf{I}_N \otimes R)\dot{\eta}(t). \tag{20}$$

Then, from Lemma 1, we have

$$\dot{V}_3 \le -\phi_1^T(\mathbf{I}_N \otimes R)\phi_1 - \phi_2^T(\mathbf{I}_N \otimes R)\phi_2 - \phi_1^T(\mathbf{I}_N \otimes S)\phi_2 - \phi_2^T(\mathbf{I}_N \otimes S^T)\phi_1 + h^2\dot{\eta}^T(t)(\mathbf{I}_N \otimes R)\dot{\eta}(t). \tag{21}$$

Let $\bar{\xi}(t) = \left[\eta(t)^T \ \eta(t-\tau)^T \ \eta(t-h)^T \ \mathbf{e}(t-\tau)^T\bar{\mathbf{e}}(t-\tau)^T\right]^T$ and $\bar{\zeta} = [\mathbf{I}_N \otimes A \ \mathbf{I}_N \otimes BK \ 0 \ \mathbf{I}_N \otimes BK \ L_{ff}^{-1}\mathcal{A}_f \otimes B]$. Then, the closed-loop dynamics (9) can be expressed as $\dot{\eta}(t) = \zeta\xi(t)$, and $\dot{V}_3$ is upper bounded by

$$\dot{V}_3 \le -\phi_1^T(\mathbf{I}_N \otimes R)\phi_1 - \phi_2^T(\mathbf{I}_N \otimes R)\phi_2 - \phi_1^T(\mathbf{I}_N \otimes S)\phi_2 - \phi_2^T(\mathbf{I}_N \otimes S^T)\phi_1 + h^2\xi(t)^T(\zeta^T(\mathbf{I}_N \otimes R)\zeta)\xi(t). \tag{22}$$

Combining results from $\dot{V}_1$, $\dot{V}_2$, and $\dot{V}_3$, we have

$$\dot{V} \le \xi^T(t)\Omega\xi(t) + h^2\xi(t)^T(\zeta^T(\mathbf{I}_N \otimes R)\zeta)\xi(t) \tag{23}$$

where

$$\Omega = \begin{bmatrix} \Omega_{11} & * & * & * & * \\ \Omega_{21} & \Omega_{22} & * & * & * \\ \Omega_{31} & \Omega_{32} & \Omega_{33} & * & * \\ \Omega_{41} & 0 & 0 & 0 & * \\ \Omega_{51} & 0 & 0 & 0 & 0 \end{bmatrix} \tag{24}$$

with

$$\Omega_{11} = \mathbf{I}_N \otimes (A^TP + PA + Q - R)$$
$$\Omega_{21} = L_{ff}^T \otimes K^TB^TP + \mathbf{I}_N \otimes (R - S^T)$$
$$\Omega_{22} = \mathbf{I}_N \otimes (-2R + S + S^T)$$
$$\Omega_{31} = \mathbf{I}_N \otimes S^T$$
$$\Omega_{32} = \mathbf{I}_N \otimes (R - S^T)$$
$$\Omega_{33} = -\mathbf{I}_N \otimes (Q + R)$$
$$\Omega_{41} = \mathbf{I}_N \otimes K^TB^TP$$
$$\Omega_{51} = \mathcal{A}_f^T L_{ff}^{-T} \otimes B^TP.$$

In addition, the inequality (14) can be rewritten as

$$\xi^T(t)\bar{\Omega}\xi(t) \le N\epsilon^2 \tag{25}$$

where

$$\bar{\Omega} = \begin{bmatrix} 0 & * & * & * & * \\ 0 & \bar{\Omega}_{22} & * & * & * \\ 0 & 0 & 0 & * & * \\ 0 & \bar{\Omega}_{42} & 0 & \bar{\Omega}_{44} & * \\ 0 & 0 & 0 & 0 & \bar{\Omega}_{55} \end{bmatrix} \tag{26}$$

with

$$\bar{\Omega}_{22} = -L_{ff}^T L_{ff} \otimes \Phi$$
$$\bar{\Omega}_{42} = -L_{ff}^T L_{ff} \otimes \Phi$$
$$\bar{\Omega}_{44} = \mathbf{I}_N \otimes \Psi_1 - L_{ff}^T L_{ff} \otimes \Phi$$
$$\bar{\Omega}_{55} = \mathbf{I}_N \otimes \Psi_2.$$

Then, using (25), $\dot{V}$ in (23) can be enlarged and rewritten as

$$\dot{V} \leq \xi(t)^T \Xi \xi(t) - \beta \eta^T \eta + N\epsilon^2 \tag{27}$$

where β is a positive constant and

$$\Xi = \Omega - \bar{\Omega} + h^2 \zeta^T (\mathbf{I}_N \otimes R)\zeta + \beta E_1^T E_1 \tag{28}$$

with $E_1 = \begin{bmatrix} \mathbf{I}_{Nn} & 0_{Nn} & 0_{Nn} & 0_{Nn} & 0_{Nn} \end{bmatrix}$. It can be shown that the formation error η will be ultimately bounded as (16) if $\Xi \leq 0$, by repeatedly using the Schur complement [24], which is equivalent to

$$\begin{bmatrix} \Omega - \bar{\Omega} & * & * \\ h(\mathbf{I}_N \otimes R)\zeta & -\mathbf{I}_N \otimes R & * \\ E_1 & 0 & -\frac{1}{\beta}\mathbf{I}_{Nn} \end{bmatrix} < 0. \tag{29}$$

We pre- and postmultiply the inequality (29) by $\text{diag}\{\mathbf{I}_N \otimes \tilde{P}, \mathbf{I}_N \otimes \tilde{P}, \mathbf{I}_N \otimes \tilde{P}, \mathbf{I}_N \otimes \tilde{P}, \mathbf{I}_N \otimes \tilde{P}, \mathbf{I}_N \otimes R^{-1}, \mathbf{I}_{Nn}\}$, where $\tilde{P} = P^{-1}$. In addition, define $\tilde{Q} = \tilde{P}Q\tilde{P}$. $\tilde{R}, \tilde{S}, \tilde{\Psi}_1, \tilde{\Psi}_2$, $\tilde{\Phi}$, and $\tilde{M}$ are defined analogously. Then, by applying the Schur complement again, the inequality in (29) is equivalent to

$$\begin{bmatrix} \tilde{\Omega} & * & * \\ h\zeta(\mathbf{I}_N \otimes \tilde{P}) & -\mathbf{I}_N \otimes R^{-1} & * \\ E_1(\mathbf{I}_N \otimes \tilde{P}) & 0 & -\frac{1}{\beta}\mathbf{I}_{Nn} \end{bmatrix} < 0 \tag{30}$$

where

$$\tilde{\Omega}_{11} = \mathbf{I}_N \otimes (\tilde{P}A^T + A\tilde{P} + \tilde{Q} - \tilde{R})$$
$$\tilde{\Omega}_{21} = \mathbf{I}_N \otimes \tilde{P}K^T B^T + \mathbf{I}_N \otimes (\tilde{R} - \tilde{S}^T)$$
$$\tilde{\Omega}_{22} = \mathbf{I}_N \otimes (-2\tilde{R} + \tilde{S} + \tilde{S}^T) + (L_{ff}^T L_{ff} \otimes \tilde{\Phi})$$
$$\tilde{\Omega}_{31} = \mathbf{I}_N \otimes \tilde{S}^T$$
$$\tilde{\Omega}_{32} = \mathbf{I}_N \otimes (\tilde{R} - \tilde{S}^T)$$
$$\tilde{\Omega}_{33} = -\mathbf{I}_N \otimes (\tilde{Q} + \tilde{R})$$
$$\tilde{\Omega}_{41} = \mathbf{I}_N \otimes \tilde{P}K^T B^T$$
$$\tilde{\Omega}_{42} = L_{ff}^T L_{ff} \otimes \tilde{\Phi}$$
$$\tilde{\Omega}_{44} = -\mathbf{I}_N \otimes \tilde{\Psi}_1 + L_{ff}^T L_{ff} \otimes \tilde{\Phi}$$

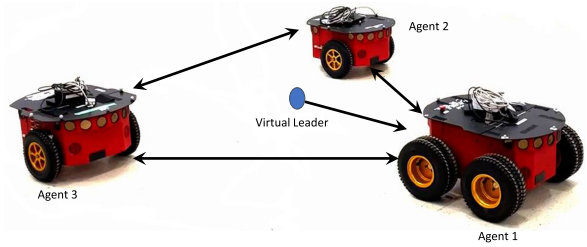

Fig. 1. Communication topology of the mobile robot team.

$$\tilde{\Omega}_{51} = \mathcal{A}_f^T L_{ff}^{-T} \otimes \tilde{P}B^T$$
$$\tilde{\Omega}_{55} = -\mathbf{I}_N \otimes \tilde{\Psi}_2.$$

Furthermore, following from the fact that $-\mathbf{I}_N \otimes R^{-1} \leq \rho^2 \mathbf{I}_N \otimes \tilde{R} - 2\rho(\mathbf{I}_N \otimes \tilde{P})$ for any positive constant $\rho > 0$, it is sufficient to ensure the inequality in (30) if

$$\begin{bmatrix} \tilde{\Omega} & * & * \\ h\zeta(\mathbf{I}_N \otimes \tilde{P}) & \rho^2 \mathbf{I}_N \otimes \tilde{R} - 2\rho(\mathbf{I}_N \otimes \tilde{P}) & * \\ E_1(\mathbf{I}_N \otimes \tilde{P}) & 0 & -\frac{1}{\beta}\mathbf{I}_{Nn} \end{bmatrix} < 0 \tag{31}$$

which is equivalent to $H < 0$ in (15) when $Y = K\tilde{P}$.

Remark 4: As shown in (16), the ultimate formation error bound is proportional to ϵ. Generally, using a larger ϵ value in the triggering functions will result in a degraded system performance while producing fewer triggering instants. Therefore, there is a tradeoff between system performance and communication usage when choosing the triggering threshold.

Remark 5: The underlying assumption of sampling synchronization across all agents poses a limitation of the developed method. In practical applications, distributed clock synchronization algorithms [25] can be applied to synchronize the clocks across multiple agents. In addition to distributedly synchronizing the agents' clocks, it is also possible to design formation controllers that are robust to sampling asynchronization.

IV. Simulation and Experimental Results

In this section, the proposed formation tracking algorithm is implemented in both simulation and experiment on a group of three unicycle-type mobile robots with a virtual leader under the communication topology shown in Fig. 1. The linearized unicycle model [26] can be expressed by (1) with $A = \begin{bmatrix} 0 & 0 \\ 0 & 0 \end{bmatrix}$ and $B = \begin{bmatrix} 1 & 0 \\ 0 & 1 \end{bmatrix}$. The desired group formation is defined by the formation vectors $f_1 = \begin{bmatrix} 1 & 0 \end{bmatrix}^T$, $f_2 = \begin{bmatrix} -0.7 & 0.7 \end{bmatrix}^T$, and $f_3 = \begin{bmatrix} -0.7 & -0.7 \end{bmatrix}^T$. It can be verified that the formation feasibility condition in Assumption 2 is satisfied with defined formation vectors. In a 14-s simulation/experiment run, the virtual leader moves at a constant speed of 0.3 m/s in the X-direction from the origin, and all followers were initially distributed near the origin. By choosing a sampling interval $h = 0.1$ s, an linear

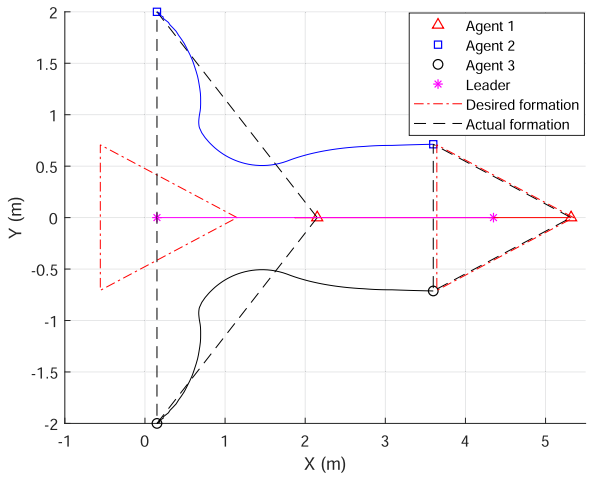

Fig. 2. Simulation results of formation evolution of the mobile robot team.

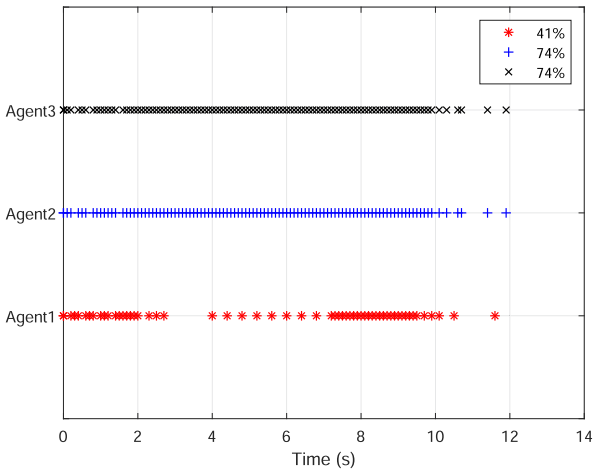

Fig. 3. Simulation results of triggering instants using estimate-based ECM.

matrix inequality (LMI) parameter $\rho = 1.5198$, and evaluating the feasibility of (15), the control gain matrix K and event generator gain matrices Φ_1, Φ_2, and Ψ can then be computed as

$$K = \begin{bmatrix} -1.0347 & 0 \\ 0 & -1.0347 \end{bmatrix}, \Phi = \begin{bmatrix} 0.0011 & 0 \\ 0 & 0.0011 \end{bmatrix}$$

$$\Psi_1 = \begin{bmatrix} 0.4087 & 0 \\ 0 & 0.4087 \end{bmatrix}, \Psi_2 = \begin{bmatrix} 1.8022 & 0 \\ 0 & 1.8022 \end{bmatrix}.$$

In addition, the triggering threshold ϵ in (11) was empirically chosen as 0.0005.

A. Simulation Results

Fig. 2 shows the simulated evolution of all agents under the proposed estimate-based controller (5) and event generator (12). The triggered communication events for all agents are depicted in Fig. 3, which shows that the average communication triggering percentage on Agents 1–3 are 41%, 74%, and 74%, respectively. To illustrate the advantages of the proposed method, similar simulations were also conducted using the state-error-based ECM [18] and a 10-Hz periodic communication mechanism. Table I summarizes the l_2 norm of all agents under the different communication mechanisms. It can be observed that the state-error-based ECM generally produces the largest l_2 norms (thus, the worst performance) under similar simulation conditions. In addition, Table II summarizes the communication triggering percentage on each agent under the different communication mechanisms and shows that the proposed estimate-error-based ECM entailed the least amount of communication resources.

TABLE I
SIMULATION RESULTS OF l_2 NORM OF FORMATION ERROR (M) OF FOLLOWER AGENTS

Mechanisms	Agent 1	Agent 2	Agent 3
Estimate-error-based ECM	0.87	2.18	2.18
State-error-based ECM	0.90	2.32	2.32
PCM	0.88	2.17	2.17

TABLE II
SIMULATION RESULTS OF TRIGGERING PERCENTAGE OF ALL AGENTS

Mechanisms	Agent 1	Agent 2	Agent 3
Estimate-error-based ECM	41	74	74
State-error-based ECM	69	72	72
PCM	100	100	100

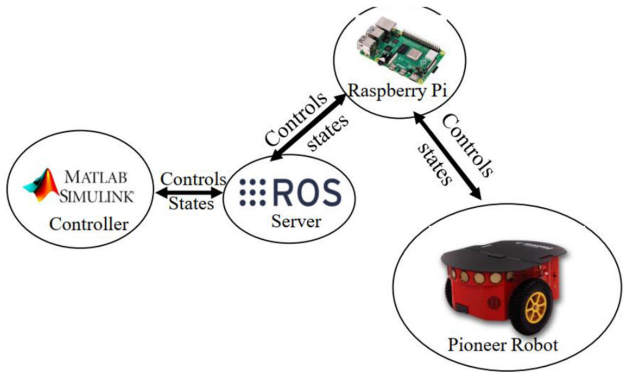

Fig. 4. Control architecture of a single Pioneer robot.

B. Experimental Results

The developed distributed event-triggered formation control algorithm was validated in a centralized manner using a group of Pioneer robots (see Fig. 1) from the host lab in the robot operating system (ROS) environment. The control algorithm was programmed in MATLAB/Simulink and integrated to the ROS network using MATLAB's Robotics Toolbox, and the Pioneer robots were integrated in the same ROS network through Raspberry Pi computers. Fig. 4 shows the control architecture for a single Pioneer robot in the ROS environment. Fig. 5 shows the time evolution of the Pioneer robots under the proposed controller (5) and event generator (12). Fig. 6 depicts the snapshots of the Pioneer group formation at $t = 0, 4.6, 9.3$, and 14 s,

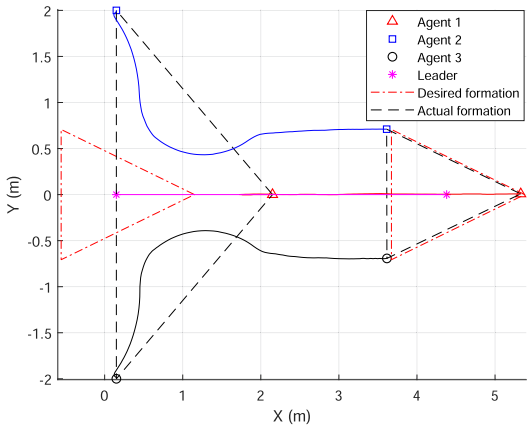

Fig. 5. Experimental results of formation evolution of the mobile robot team.

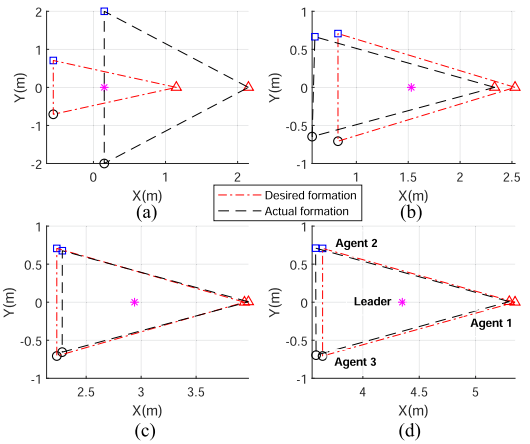

Fig. 6. Experimental results of snapshots of the mobile robot team in the X–Y plane at: (a) $t = 0$ s, (b) $t = 4.6$ s, (c) $t = 9.3$ s, and (d) $t = 14$ s.

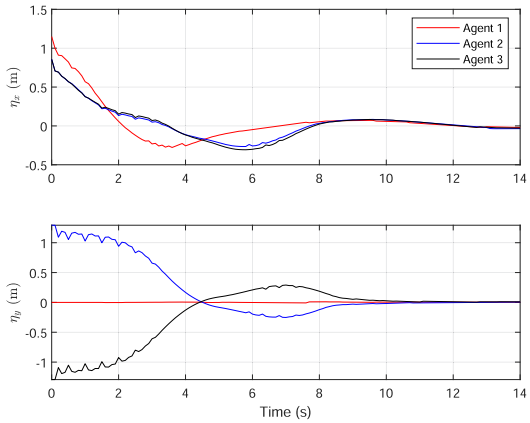

Fig. 7. Experimental results of formation error in X- and Y-directions.

respectively. Fig. 7 demonstrates the formation error evolution for each agent in the X- and Y-directions. The communication instants on each Pioneer robot are illustrated in Fig. 8, which clearly shows that the communication events were sparsely distributed as the system approaches the desired formation. In contrast, the communication instants under the conventional

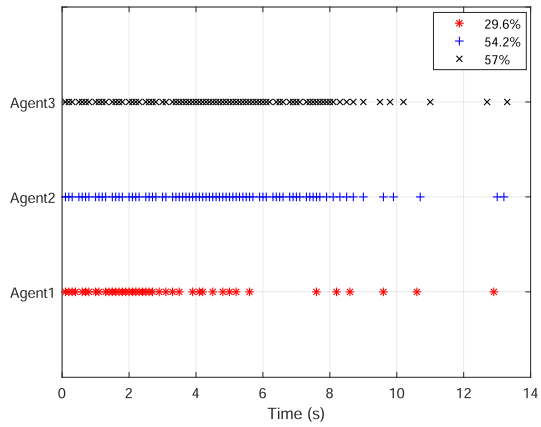

Fig. 8. Experimental results of triggering instants using estimate-based ECM.

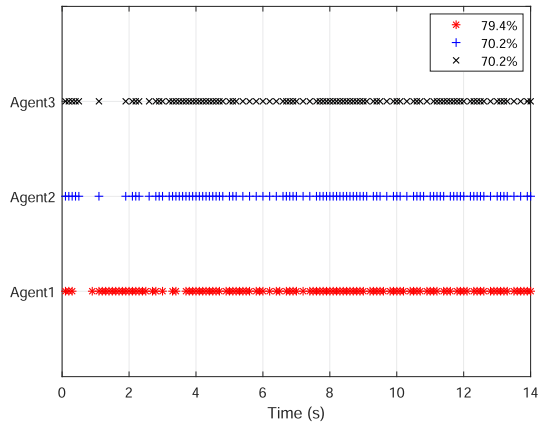

Fig. 9. Experimental results of triggering instants using state-based ECM.

TABLE III
EXPERIMENTAL RESULTS OF l_2 NORM OF FORMATION ERROR (m) OF FOLLOWER AGENTS

Mechanisms	Agent 1	Agent 2	Agent 3
Estimate-error-based ECM	1.01	2.08	2.08
State-error-based ECM	1.12	2.37	2.40
PCM	1.01	2.04	2.05

TABLE IV
EXPERIMENTAL RESULTS OF TRIGGERING PERCENTAGE OF ALL AGENTS

Mechanisms	Agent 1	Agent 2	Agent 3
Estimate-error-based ECM	30	54	57
State-error-based ECM	80	70	70
PCM	100	100	100

state-error-based ECM in Fig. 9 were still densely gathered when the desired group formation was approached. The l_2 norm of formation errors and communication triggering percentage of all Pioneer agents under the three communication mechanisms are summarized in Tables III and IV, which conclude that the experimental results follow the same trends as the simulation results—with the newly proposed estimate-error-based ECM able to produce comparable performance while entailing the least amount of communication resources.

V. Conclusion

In this article, the distributed leader–follower formation tracking control problem for a networked MAS with general linear agents was investigated under a sampled-data setting. A novel locally computable event-triggered broadcasting mechanism was proposed to regulate the data transmission in each follower agent. A new distributed formation controller was then designed based on the event-generator-regulated information. For the conditions used in this research, both simulation and experiment results show that the proposed approach can generate less communication instants while still producing a comparable performance.

References

[1] W. Ren and Y. Cao, *Distributed Coordination of Multi-Agent Networks: Emergent Problems, Models, and Issues*. London, U.K.: Springer, 2010.

[2] M. A. Lewis and K.-H. Tan, "High precision formation control of mobile robots using virtual structures," *Auton. Robots*, vol. 4, no. 4, pp. 387–403, 1997.

[3] P. K. Wang, "Navigation strategies for multiple autonomous mobile robots moving in formation," *J. Robot. Syst.*, vol. 8, no. 2, pp. 177–195, 1991.

[4] W. Ren and N. Sorensen, "Distributed coordination architecture for multi-robot formation control," *Robot. Auton. Syst.*, vol. 56, no. 4, pp. 324–333, 2008.

[5] K.-K. Oh, M.-C. Park, and H.-S. Ahn, "A survey of multi-agent formation control," *Automatica*, vol. 53, pp. 424–440, 2015.

[6] Y. Hua, X. Dong, Q. Li, and Z. Ren, "Distributed time-varying formation robust tracking for general linear multiagent systems with parameter uncertainties and external disturbances," *IEEE Trans. Cybern.*, vol. 47, no. 8, pp. 1959–1969, Aug. 2017.

[7] D. Li, S. S. Ge, W. He, C. Li, and G. Ma, "Distributed formation control of multiple Euler-Lagrange systems: A multilayer framework," *IEEE Trans. Cybern.*, to be published, doi: 10.1109/TCYB.2020.3022535.

[8] H. Du, W. Zhu, G. Wen, and D. Wu, "Finite-time formation control for a group of quadrotor aircraft," *Aerosp. Sci. Technol.*, vol. 69, pp. 609–616, 2017.

[9] X. Dong and G. Hu, "Time-varying formation control for general linear multi-agent systems with switching directed topologies," *Automatica*, vol. 73, pp. 47–55, 2016.

[10] Y. Hua, X. Dong, G. Hu, Q. Li, and Z. Ren, "Distributed time-varying output formation tracking for heterogeneous linear multiagent systems with a nonautonomous leader of unknown input," *IEEE Trans. Autom. Control*, vol. 64, no. 10, pp. 4292–4299, Oct. 2019.

[11] D. V. Dimarogonas, E. Frazzoli, and K. H. Johansson, "Distributed event-triggered control for multi-agent systems," *IEEE Trans. Autom. Control*, vol. 57, no. 5, pp. 1291–1297, May 2012.

[12] L. Ding, Q.-L. Han, X. Ge, and X.-M. Zhang, "An overview of recent advances in event-triggered consensus of multiagent systems," *IEEE Trans. Cybern.*, vol. 48, no. 4, pp. 1110–1123, Apr. 2018.

[13] C. Nowzari, E. Garcia, and J. Cortés, "Event-triggered communication and control of networked systems for multi-agent consensus," *Automatica*, vol. 105, pp. 1–27, 2019.

[14] E. Garcia, Y. Cao, and D. W. Casbeer, "An event-triggered control approach for the leader-tracking problem with heterogeneous agents," *Int. J. Control*, vol. 91, no. 5, pp. 1209–1221, 2018.

[15] X. Li, Y. Tang, and H. R. Karimi, "Consensus of multi-agent systems via fully distributed event-triggered control," *Automatica*, vol. 116, 2020, Art. no. 108898.

[16] X. Yin, D. Yue, and S. Hu, "Adaptive periodic event-triggered consensus for multi-agent systems subject to input saturation," *Int. J. Control*, vol. 89, no. 4, pp. 653–667, 2016.

[17] E. Garcia, Y. Cao, and D. W. Casbeer, "Cooperative control with general linear dynamics and limited communication: Centralized and decentralized event-triggered control strategies," in *Proc. Amer. Control Conf.*, 2014, pp. 159–164.

[18] X. Ge and Q.-L. Han, "Distributed formation control of networked multi-agent systems using a dynamic event-triggered communication mechanism," *IEEE Trans. Ind. Electron.*, vol. 64, no. 10, pp. 8118–8127, Oct. 2017.

[19] G. Guo, L. Ding, and Q.-L. Han, "A distributed event-triggered transmission strategy for sampled-data consensus of multi-agent systems," *Automatica*, vol. 50, no. 5, pp. 1489–1496, 2014.

[20] P. Park, J. W. Ko, and C. Jeong, "Reciprocally convex approach to stability of systems with time-varying delays," *Automatica*, vol. 47, no. 1, pp. 235–238, 2011.

[21] Z. Huang, Y.-J. Pan, and R. Bauer, "Formation control with dynamic non-autonomous leader using sampled-data event-triggered communication," in *Proc. Amer. Control Conf.*, 2021, pp. 2643–2648.

[22] Y. Fan, G. Feng, Y. Wang, and C. Song, "Distributed event-triggered control of multi-agent systems with combinational measurements," *Automatica*, vol. 49, no. 2, pp. 671–675, 2013.

[23] C. Peng, J. Zhang, and Q.-L. Han, "Consensus of multiagent systems with nonlinear dynamics using an integrated sampled-data-based event-triggered communication scheme," *IEEE Trans. Syst., Man, Cybern. Syst.*, vol. 49, no. 3, pp. 589–599, Mar. 2019.

[24] J. G. Van Antwerp and R. D. Braatz, "A tutorial on linear and bilinear matrix inequalities," *J. Process Control*, vol. 10, no. 4, pp. 363–385, 2000.

[25] L. Schenato and F. Fiorentin, "Average TimeSynch: A consensus-based protocol for clock synchronization in wireless sensor networks," *Automatica*, vol. 47, no. 9, pp. 1878–1886, 2011.

[26] L. Sheng, Y.-J. Pan, and X. Gong, "Consensus formation control for a class of networked multiple mobile robot systems," *J. Control Sci. Eng.*, vol. 2012, 2012, Art. no. 1.

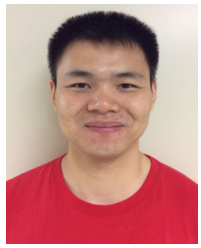

Zipeng Huang (Student Member, IEEE) received the B.E. and M.A.Sc. degrees, in 2015, and 2017, respectively, from the Department of Mechanical Engineering, Dalhousie University, Halifax, NS, Canada, where he currently working toward the Ph.D degree, all in mechanical engineering.

His research interests include nonlinear systems, multiagent systems, mechatronics, and robotics.

Robert Bauer received the B.A.Sc. degree in mechanical engineering from the University of Waterloo, Waterloo, ON, Canada, in 1994, and the Ph.D. degree from the University of Toronto Institute for Aerospace Studies, Toronto, ON, Canada, in 1998.

He is currently a Professor with the Department of Mechanical Engineering, Dalhousie University, Halifax, NS, Canada. His research interests include robotics, system dynamics modelling, and control fields for aerospace, oceans, and manufacturing applications.

Ya-Jun Pan (Senior Member, IEEE) received the B.E. degree in mechanical engineering from Yanshan University, Qinhuangdao, China, in 1996, the M.E. degree in mechanical engineering from Zhejiang University, Hangzhou, China, in 1999, and the Ph.D. degree in electrical and computer engineering from the National University of Singapore, Singapore, in 2003.

She is currently a Professor with the Department of Mechanical Engineering, Dalhousie University, Halifax, NS, Canada. She was a Postdoc with the Laboratoire d'Automatique de Grenoble (GIPSA-Lab), Centre National De La Recherche Scientifique, Paris, France, in 2003 and the Department of Electrical and Computer Engineering, University of Alberta, Edmonton, AB, Canada, in 2004. Her research interests include robust nonlinear control, cyber physical systems, intelligent transportation systems, haptics, and collaborative multiple robotic systems.

Prof. Pan is currently an Associate Editor for the IEEE Transactions on Cybernetics, and was an Associate Editors for the IEEE/ASME Transactions on Mechatronics and IEEE Transactions on Industrial Electronics. She is a Fellow of the Engineering Institute of Canada and ASME, and a registered Professional Engineer in Nova Scotia, Canada.